RSC Advances

ROYAL SOCIETY OF CHEMISTRY

www.rsc.org/advances

Journal Name

ARTICLE

Synthesis of Nd^{3+}/Yb^{3+} Sensitized Upconversion Core-shell Nanocrystals with Optimized Hosts and Doping Concentrations†

Received 00th January 20xx,
Accepted 00th January 20xx

DOI: 10.1039/x0xx00000x

www.rsc.org/

Kun Wang,[a] Wanli Qincheng,[a] Yong Zhang,[b]* Ru Qiao,[b] Sheng Li[a] and Zhengquan Li*[ab]

Development of upconversion nanocrystals (UCNs) under 808nm excitation other than 980nm is much important to biological applications for avoiding tissue over-heating. Nd^{3+} and Yb^{3+} dual-sensitized UCNs are proven to be promising candidates but how to select host materials to construct core-shell UCNs with strong UC emissions still remains unexplored. Herein, we prepare a series of homogenous and heterogeneous core-shell UCNs using $NaYF_4$ and $NaGdF_4$ as the core-host and/or as the shell-host, respectively, through the seed-mediate synthetic approach. Our results show that selecting the core-host in the core-shell UCNs plays the key role in determining their final UC intensities. Furthermore, homogenous core-shell UCNs can give stronger UC fluorescence than the heterogeneous ones due to the low crystal defects at the core-shell interface. Moreover, the concentration effect of activator ions and sensitizer ions in these core-shell UCNs on their UC emissions is analyzed, and optimal doping under different NIR excitation (808nm, 980nm or 808nm/980nm) is achieved.

Introduction

Lanthanide nanocrystals (NCs) with upconversion (UC) fluorescence have attracted extensive research interests in the past decade.[1-10] Owing to their unique upconverting properties and other features such as narrow emissions, long luminescence lifetimes, and high photostability, upconversion nanocrystals (UCNs) have shown potential applications in a variety of fields including imaging, sensing, drug delivery, and photodynamic therapy.[11-16] Typically, a UCN is constituted by the host nanomatrix which is simultaneously doped with sensitizer ions (usually Yb^{3+}) and activator ions (Er^{3+}, Tm^{3+}, or Ho^{3+} etc.).[17-19] The sensitizer ions continuously absorb near-infrared (NIR) photons and then transfers energy to the activator ions for luminescence. Although great advances have been made in the past years, recent progress on UCNs has been largely hindered because most of the developed UCNs are sensitized by Yb^{3+} ions which only respond to a narrow-band NIR excitation centered at 980nm. The absorption of Yb^{3+} ions overlaps the maximal absorption of water molecules that are dominant in biological samples. Over-exposure of bio-species under 980nm diode laser may induce potential thermal damages to cells and tissues due to over-heating, limiting these UCNs for deep tissue imaging. To address this issue, exploration of new sensitized UCNs which can absorb other NIR bands in addition to 980nm is an elegant solution. In searching of this type of sensitizer ions, Nd^{3+} has been proven to be a good choice because Nd^{3+} doped UCNs exhibits intense absorption around 808nm at which water absorption is minimal. Furthermore, Nd^{3+} has a larger absorption cross-section in the NIR region than that of Yb^{3+}.[20] Particularly, it has been revealed that the energy transfer of $Nd^{3+}\rightarrow Yb^{3+}$ has a high efficiency in many types of host materials,[21-26] suggesting that co-doping of Nd^{3+} and Yb^{3+} is a practical approach to develop new types of UCNs under the excitation of 808nm.

Recently, several attempts have been made to the synthesis of Nd^{3+} sensitized UCNs which show impressive UC emission under 808nm excitation. For examples, Han et al. pioneered the synthesis of Yb/Er/Nd triply doped $NaYF_4$ NCs which can be excited under 808nm.[22] However, the deleterious cross-relaxation between activator ions and Nd^{3+} ions requires low Nd^{3+} doping concentration (typically < 2%), which leads to weak absorption at 808nm and low UC emissions. To increase the Nd^{3+} doping, core-shell structured NCs (such as $NaGdF_4$@$NaGdF_4$ and $NaYF_4$@$NaYF_4$) were developed by Yan's group and Liu's group, respectively.[20,23] In such configuration, the activators ions and Nd^{3+} ions can be spatially separated in a single particle and thus serous cross-relaxation are suppressed. Very recently, Wang et al also reported a four-layered core-shell $NaGdF_4$ NCs which can emit both down- and up-conversion emissions at single 808nm excitation.[24] All above works have shown important insights into the design and synthesis of Nd^{3+} sensitized UCNs under the NIR band at 808nm.

Despite above progress, there are still a few questions remains unexplored and deserve further investigation. First, either $NaYF_4$ or $NaGdF_4$ was monotonously used as host materials in these developed core-shell UCNs.[20-24] Considering

[a] Department of Materials Physics, Zhejiang Normal University, Jinhua, Zhejiang 321004, P. R. China.
[b] Institute of Physical Chemistry, Zhejiang Normal University, Jinhua, Zhejiang 321004, P. R. China.
† Electronic Supplementary Information (ESI) available: size distributions and UC emissions of the seeds and core-shell UCNs. See DOI: 10.1039/x0xx00000x

that both of them are excellent host matrixes for UC luminescence upon lanthanide doping, which kind of core-shell configuration is the best if homogeneous core-shell hosts ($NaLn(1)F_4$@$NaLn(1)F_4$) and heterogeneous core-shell hosts ($NaLn(1)F_4$@$NaLn(2)F_4$) are compared (Ln(1) and Ln(2) mean different lanthanide elements)? Second, when referring to the synthesis of dual Nd^{3+}/Yb^{3+} sensitized UCN aiming to be excited at both 808nm and 980nm, how to control the doping concentrations of sensitizer ions in the shell and activator ions in the core?

To clarify above issues, herein we employ a seed-mediate synthetic approach to prepare both homogenous core-shell NCs (e.g., $NaYF_4$@$NaYF_4$ and $NaGdF_4$@$NaGdF_4$) and heterogeneous core-shell NCs (e.g., $NaYF_4$@$NaGdF_4$ and $NaGdF_4$@$NaYF_4$). After doping different amounts of activator and/or sensitizer ions, we have systematically investigated the UC emissions from these core-shell UCNs under 808nm and 980nm excitation, respectively. Our results show that selecting nanohosts for the core play a key role in determining the final UC emissions of these core-shell UCNs. Furthermore, it is found that homogenous core-shell structure is better than the heterogonous one due to low crystal defects at the interface between the core and the shell. Moreover, doping effects of the activator ions in the core and sensitizer ions in the shell have been tested, and an optimal doping concentration is achieved in the core-shell UCNs. This work may shed some new lights on the design and synthesis of dual Nd^{3+}/Yb^{3+} sensitized UCNs with a core-shell configuration.

Experimental section

Synthesis of the core-shell structured UCNs

High-quality $NaYF_4$:Yb(20%),Tm(0.5%) NCs were synthesized using a user-friendly method we have previously developed.[27] To prepare core-shell structured $NaYF_4$:Yb,Tm@$NaYF_4$:Yb,Nd (termed as Y@Y) NCs, the $NaYF_4$:Yb (20%),Tm(0.5%) NCs were used as seeds to epitaxial grow a $NaYF_4$:Yb(10%), Nd(10%) layer on their surface.[28] In a typical synthesis, 0.8 mmol YCl_3, 0.1 mmol $YbCl_3$ and 0.1 mmol $NdCl_3$ were mixed with 6 mL oleic acid and 15 mL 1-octadecene in a 50-mL flask. The solution was heated to 160 °C to form a homogeneous solution, and then cooled down to 70 °C. 1 mmol $NaYF_4$:Yb(20%),Tm(0.5%) NCs in 10 mL cyclohexane were then added into the solution and the cyclohexane solution was gradually removed upon evaporation. After that, 10 mL methanol solution containing 4 mmol NH_4F and 2.5 mmol NaOH was added and stirred for 30 min. Subsequently, the solution was slowly heated to remove methanol, degassed at 100 °C for 10 min, and then heated to 300 °C and maintained for 1h under Ar protection. After the solution was cooled down to room temperature naturally, the products were precipitated from the solution with ethanol, and washed with ethanol/cyclohexane (1:1 v/v) for three times. Finally, the prepared core-shell NCs was dispersed in 10 ml cyclohexane for further use.

The $NaGdF_4$:Yb,Tm NCs were prepared with the similar protocol to the synthesis of $NaYF_4$:Yb,Tm NCs. Other core-shell NCs such as $NaYF_4$:Yb,Tm@$NaGdF_4$:Yb,Nd, $NaGdF_4$:Yb,Tm@$NaGdF_4$:Yb,Nd and $NaGdF_4$:Yb,Tm@ $NaYF_4$:Yb,Nd (termed as Y@Gd, Gd@Gd and Gd@Y), were also prepared according the seed-mediate approach as the synthesis of Y@Y.

Characterizations

The morphologies of samples were observed by transmission electron microscopy (TEM) which was taken on a JEOL 2010F TEM operating at 200 kV. The TEM samples were prepared by dropping a suspension of NCs on a carbon-film coated copper grid. X-ray powder diffraction (XRD) was carried out on a Japan Rigaku D/max rA X-ray diffractometer equipped with a Cu Kα radiation. X-ray photoelectron spectra (XPS) were collected on an ESCAlab MKII X-ray photoelectron spectrometer. Fluorescence spectra were acquired on a Hitachi F-7000 spectrometer equipped with commercial 980nm and 808nm NIR laser, respectively. Size distribution of the NCs was obtained using a Malvern Zetasizer Nano (ZEN3690).

Results and discussion

TEM characterizations of the core-shell NPs

TEM image of the prepared $NaYF_4$:Yb,Tm NCs are as shown in Figure 1A. These NCs are uniform in size with a diameter of 32 nm. When these NCs were used as seeds, an layer of $NaYF_4$:Yb,Nd can be epitaxial grown on the seeded NCs. As a result, core-shell Y@Y with different dopants in the core and the shell are produced. From the TEM image (Figure 1B), one can see that the size of the Y@Y NCs has increased to 40 nm and the structural uniformity of the core-shell NCs is reserved as the core NCs. Using the similar protocol, an $NaGdF_4$:Yb,Nd shell can also be produced on the seeded $NaYF_4$:Yb,Tm NCs (Figure 1C), because $NaGdF_4$ and $NaYF_4$ crystals have the same crystal structure (hexagonal phase) and growing habits during the synthesis. This kind of seed-mediate approach has been well established in the synthesis of core-shell structured lanthanide fluoride NCs.[29] Similarly, we have also prepared $NaGdF_4$:Yb,Tm NCs and epitaxial grown a $NaYF_4$:Yb,Nd shell or a $NaGdF_4$:Yb,Nd shell on them, respectively (see Figure 1D, 1E and 1F). The obtained core-shell Gd@Y and Gd@Gd NCs also exhibit uniform structures as the seeded $NaGdF_4$:Yb,Tm NCs except the incensement in particle size. Size distributions of these NCs before and after the shell growth have also been measured (see Figure S1). This result also show that both the core NCs and corresponding core-shell NCs have a narrow size distribution, confirming that a uniform shell has been produced on these core NCs. XRD patterns and XPS analyses of $NaYF_4$:Yb,Tm NCs before and after growing a $NaGdF_4$:Yb,Nd shell were also investigated. XRD data confirm that the core and the shell are much similar in phase and lattice (see Figure S2). XPS data reveal that the surface of Y@Gd NCs is dominated by element Gd (see Table S1), implying a $NaGdF_4$ was covered on $NaYF_4$:Yb,Tm NCs.

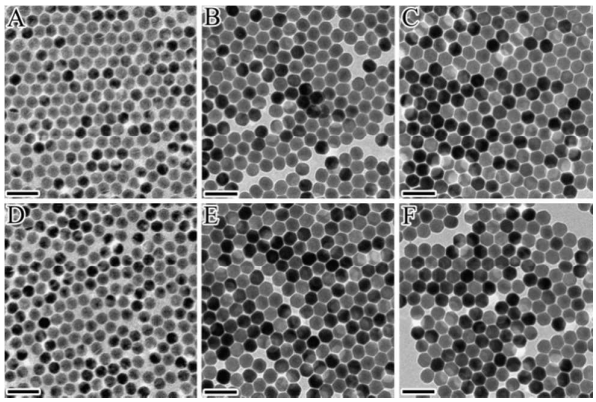

Fig. 1 TEM images of the seeded NCs and corresponding core-shell NCs: (A) $NaYF_4$; (B) $NaYF_4$@$NaYF_4$; (C) $NaYF_4$@$NaGdF_4$; (D) $NaGdF_4$; (E) $NaGdF_4$@$NaYF_4$; (F) $NaGdF_4$@$NaGdF_4$. (Scale bars: 100nm.)

UC emissions from different core-shell samples

For the Yb^{3+} sensitized UCNs (980nm), Yb^{3+} ions can effectively transfer energy to activator ions (e.g., Tm^{3+}) and avoid deleterious cross-relaxation.[30,31] Thus, Yb^{3+} and Tm^{3+} can be homogenously doped together in a single NC for UC emissions. For the Nd^{3+} sensitized UCNs (808nm), however, serous deleterious cross-relaxation appears between Nd^{3+} and Tm^{3+} ions when they are homogenously doped in one single NC.[22] To suppress the deleterious cross-relaxation, core-shell structure is required to spatially separate the Nd^{3+} ions from Tm^{3+} ions by doping them in the shell and in the core, respectively. For above consideration, core-shell structure is thus preferred for constructing dual Nd^{3+}/Yb^{3+} sensitized UCNs in our case. On the other hand, since the energy transfer (ET) of $Nd^{3+}\rightarrow Yb^{3+}\rightarrow Tm^{3+}$ is an efficient channel to give UC emissions under 808nm excitation, co-doping of Yb^{3+} ions in both the shell and the core is favorable, for the ET and sensitization purpose, respectively. UC mechanism in the dual sensitized core-shell NCs can be illustrated in Figure 2.

To investigate the host effect on the core and the shell, individually, we have prepared core-shell Y@Y, Y@Gd, Gd@Gd and Gd@Y NCs which doped with the same amount of lanthanide ions in the core (20%Yb and 0.5%Tm) and in the shell (10%Yb and 10%Nd). UC spectra of these core-shell NCs were measured and show in Figure 3A and 3B, respectively. Under either 980nm or 808nm excitation, strong emissions at 360nm, 450nm and 475nm are observed. The ultra-violet emission at 360nm and blue emission at 450nm are from four-photon processes, owing to the transitions of $^1D_2\rightarrow{}^3H_6$ and $^1D_2\rightarrow{}^3H_4$ in Tm^{3+} ions, respectively. The blue emission at 475nm is from three-photon processes due to the transition of $^1G_4\rightarrow{}^3H_6$ in Tm^{3+} ions.[32] In both UC spectra, it is observed that Y@Y NCs display the highest intensity under the same concentration and measuring condition, and the Y@Gd NCs possess the second position. In contrast, Gd@Gd and Gd@Y NCs exhibit relatively low intensity and take the third and fourth position, respectively. Note that UC intensities from these core-shell hosts are in the same sequence under either

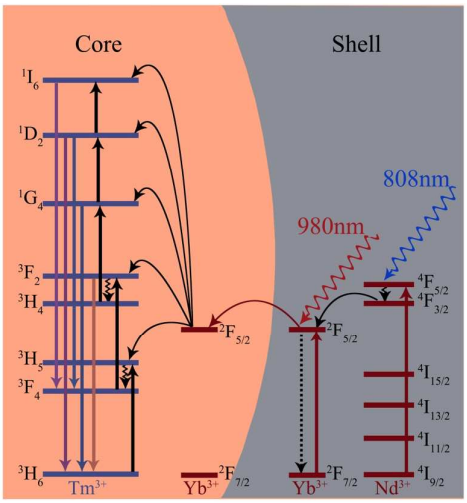

Fig. 2 Proposed energy transfer upconversion mechanism in the core-shell structured NCs.

980nm or 808nm excitation, namely, Y@Y＞Y@Gd＞Gd@Gd ＞Gd@Y.

Host effect in the core-shell UCNs

Judging from the UC intensities from above four core-shell samples, one can see that two samples prepared with $NaYF_4$:Yb,Tm cores shows stronger emissions than the other two samples prepared with $NaGdF_4$:Yb,Tm cores. This result indicates that selecting the core-host play the key role in determining their final UC intensity. In previous research, it has been revealed that both $NaYF_4$ and $NaGdF_4$ are efficient hosts for UC luminescence among the fluoride NCs when doped with Yb^{3+} and Tm^{3+} (or Er^{3+}).[33-36] Since the UC emissions are resulted from electron transitions of the activator ions, a better host for the activator ions is thus crucial for these core-shell UCNs. In our case, the seeded $NaYF_4$:Yb(20%),Tm(0.5%) NCs show stronger UC fluorescence than the seeded $NaGdF_4$:Yb(20%),Tm(0.5%) (see Figure S3). This is probably due to the fact that Yb^{3+} and Tm^{3+} doped in $NaYF_4$ may produce less crystals defects and lattice stress than those doped in $NaGdF_4$, since the ionic radius of Y^{3+} is closer to those of Yb^{3+} and Tm^{3+} than that of Gd^{3+}.[37,38] Therefore, Y@Y and Y@Gd display higher intensities than Gd@Gd and Gd@Y with the same doping concentrations.

Once the host material for the core is determined, the final UC emission intensity of sample will depend on the selection of the shell materials. Among our four core-shell samples, it is also observed that homogeneous core-shell hosts are better than the heterogeneous core-shell hosts (i.e., Y@Y>Y@Gd and Gd@Gd>Gd@Y). It means that an ideal host material for the shell does not rely on what kind of material it is but depends on what core material has already employed as the seeds in these core-shell UCNs. Selecting the same material for the shell as the core will favor better UC fluorescence under the same doping condition. It is known that crystal defects are fluorescence quenchers to lanthanide NCs. The difference

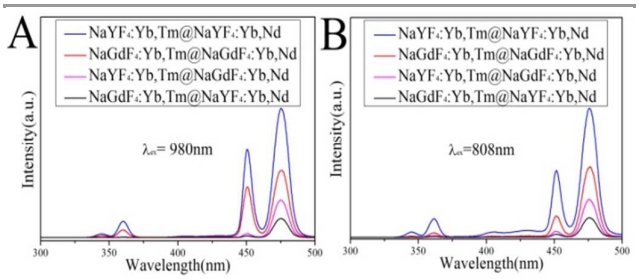

Fig. 3 UC emission spectra of four core-shell UCNs constituted by different core-host and/or shell-host with the same doping concentrations under different NIR excitation: (A) 808nm NIR laser; (B) 980nm NIR laser.

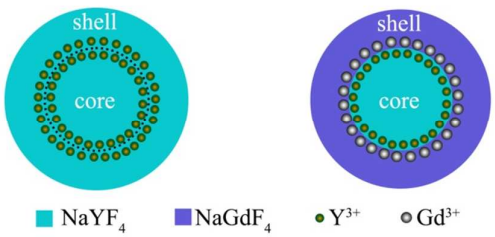

Fig. 4 Schematic illustration of the core-shell structure of a single $NaYF_4$@$NaYF_4$ and $NaYF_4$@$NaGdF_4$ NC. More crystal defects may appear at the core/shell interface of $NaYF_4$@$NaGdF_4$ NC due to the different ionic radii of Y^{3+} and Gd^{3+}.

between heterogeneous core-shell NC and homogenous core-shell NC is that there is an obvious interface between the core and the shell (see Figure 4). Obviously, more crystal defects will appear at the interface of the heterogeneous core-shell NCs because they are made by different materials despite that they have similar crystal structure (hexagonal phase). Therefore, homogeneous core-shell hosts will achieve higher intensity than heterogeneous core-shell hosts. As a result, the sequence in UC emissions is Y@Y > Y@Gd > Gd@Gd > Gd@Y. In short, the selection rule for the core-shell hosts is as follows: (1) selecting an ideal core-host for doping the activator ions; (2) selecting the same material for the shell-host as the core-host to avoid interfacial crystal defects.

Optimizing doping concentrations in the core-shell NCs

In order to reach the best UC performance, we have investigated the effect of doping concentrations of different ions on their final UC fluorescence, using the Y@Y NCs as an example. Firstly, we doped different amount of Yb^{3+} ions in the core and fixed the doping concentration of other ions. When the concentration of Yb^{3+} ions in the core increases from 10% to 15% and 20%, the total fluorescence of NCs has distinctly enhanced under the 808nm excitation (Figure 5A). This enhancement indicates that more Yb^{3+} ions can enhance the ET process from the shell to the core since Yb^{3+} does not directly absorb 808nm light. However, obvious decrease in intensity appears once the doping concentration is over 25%, suggesting that obvious cross-relaxation between Yb^{3+} ions will arise at high Yb^{3+} doping. Therefore, optimal doping concentration of Yb^{3+} is around 20% in the core for the Y@Y NCs. In the similar way, we have tried different amount of Tm^{3+} ions in the core from 0.1% to 0.8% and fixed the Yb^{3+} doping at 20% (Figure 5B). The result implies that 0.5% Tm^{3+} is the best doping level for UC luminescence and over-doping of Tm^{3+} will induce obvious cross-relaxation between the activator ions. Note that the best doping concentration of Yb^{3+} and Tm^{3+} in the core-shell NCs are similar to the optimal doping of Yb^{3+} and Tm^{3+} in the $NaYF_4$ seeds,[39] confirming that the key to strong UC fluorescence mainly relies on the performance of the core NCs. The requirement of high Yb^{3+} concentration and relatively low Tm^{3+} concentration is because the three- and four-photon UC process of Tm^{3+} ions which require sufficient energy from the surrounded sensitizer ions.

Similarly, we also optimized the doping concentration of Yb^{3+} and Nd^{3+} ions in the shell by fixing the doping ions in the core. Under 808nm excitation, the Yb^{3+} in the shell serve as a bridge to transfer energy from the Nd^{3+} ions to Tm^{3+} ions in the core. As such, too low Yb^{3+} concentration does not favor the ET process while too much Yb^{3+} ions will prolong the ET pathway and reduce the ET efficiency.[20] Therefore, there is an optimal doping concentration of Yb^{3+} in the shell host, too. The optimal level of Yb^{3+} ions is found to be 10% when the Nd^{3+} doping is fixed at 10% (a pretty high concentration for Nd^{3+}) (see Figure 5C). On the other hand, the Nd^{3+} ions serve as sensitizers to directly absorb 808nm light and then transfer energy to Yb^{3+} ions. Although core-shell configuration can suppress deleterious cross-relaxation between Tm^{3+} and Nd^{3+} to some extent, over-doping of Nd^{3+} in the shell will also enhance such cross-relaxation due to more Nd^{3+} ions will appear at the interface.[24] In the Y@Y NCs, the optimal Nd^{3+} doping for strong UC fluorescence is around 10% (see Figure 5D).

We also tested the UC fluorescence of above samples under 980nm excitation (see Figure S4). It was found that the optimal doping for Yb^{3+} and Tm^{3+} in the core is similar to the samples excited under 808nm. The difference lies in the doping concentration of Yb^{3+} ions in the shell. Under 980nm excitation, the UC intensities can be greatly improved along with the increase of Yb^{3+} concentration and the optimal doping has increases to 20%. This is because that Yb^{3+} in the shell can help to absorb 980nm light along with the Yb^{3+} doped in the core, serving as an 'active shell' in the core-shell NCs.[40] The concentration of Nd^{3+} in the shell (below 10%) has little effect on the UC emissions since they did not absorb the 980nm light.

The UC fluorescence of samples doped with various amount of ions were also evaluated under simultaneous NIR excitation of 808nm/980nm (two NIR lasers were simultaneously used with the same power) (see Figure 6). Interestingly, it is found that the optimal doping of Yb^{3+} and Tm^{3+} in the core and Nd^{3+} in the shell is similar to the samples excited under single 808nm excitation. This is because these doping ions have similar functions under either 808nm or 980nm excitation. However, a relatively higher Yb^{3+} doping in the shell (25%) is required for achieving the best UC fluorescence. This is attributed to the fact that the Yb^{3+} ions in the shell have two functions when the samples were simultaneously excited under 808nm and 980nm. They not only serve as sensitizer ions for the absorption of

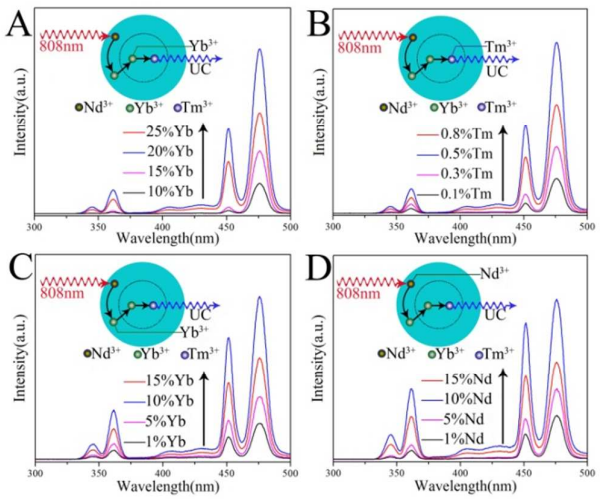

Fig. 5 Comparison of UC emission intensities of $NaYF_4$:Yb,Tm@$NaYF_4$:Yb,Nd UCNs under 808nm excitation by changing the doping concentration of different ions: (A) Yb^{3+} in the core; (B) Tm^{3+} in the core; (C) Yb^{3+} in the shell; (D) Nd^{3+} in the shell.

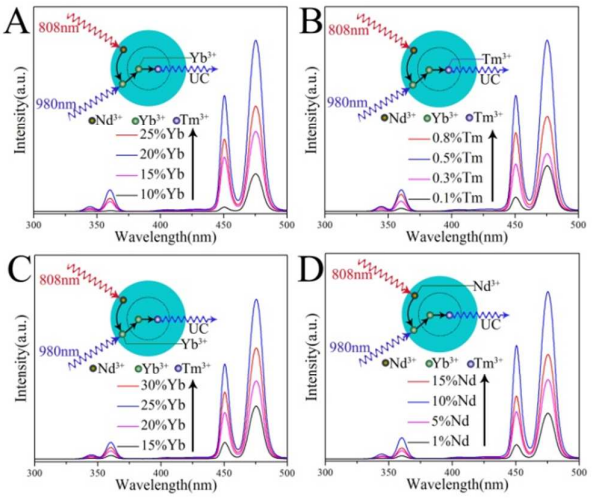

Fig. 6 Comparison of UC emission intensities of $NaYF_4$:Yb,Tm@$NaYF_4$:Yb,Nd UCNs under simultaneous 808nm/980nm excitation by changing the doping concentration of different ions: (A) Yb^{3+} in the core; (B) Tm^{3+} in the core; (C) Yb^{3+} in the shell; (D) Nd^{3+} in the shell.

980nm light but also work as energy migrators in the $Nd^{3+}\rightarrow Yb^{3+}\rightarrow Tm^{3+}$ channel at 808nm excitation. As such, the optimal Yb^{3+} doping should more than 20% for both the sensitization and ET purpose. Core-shell UCNs with excitation at two NIR bands may also have potential in the hybrid UC/semiconductor photocatalysts in addition to the biological applications, since they can show strong UC emissions under a wider NIR region.

Conclusions

In summary, we employed the seed-mediate approach and prepared a series of homogenous and heterogeneous core-shell UCNs using $NaYF_4$ and $NaGdF_4$ as core-host and/or shell-host, respectively. After lanthanide doping, the UC emissions of these samples were mechanically investigated. It is found that selecting the core-host plays the key role in determining their final UC intensities. At the same time, homogenous core-shell UCNs can give stronger UC fluorescence than the heterogeneous one due to the low crystal defects at the core-shell interface. Through doping different activator and/or sensitizer ions in the core and in the shell, we also evaluated the concentration effect of various lanthanide ions on their UC fluorescence. Optimal doping concentration under different NIR excitation (808nm, 980nm and both 808nm/980nm) is analyzed. This work may shed some new lights on the design and synthesis of core-shell lanthanide NCs with dual sensitized features.

Acknowledgements

The authors acknowledge financial support from National Nature Science Foundation of China (Nos 21273203 and 21201151) and Zhejiang Provincial Natural Science Foundation (Nos LR15B0100 01 and LR12B040001).

References

1. T. Kano, H. Yamamoto, Y. Otomo, *J. Electrochem. Soc.,* 1972, **119**, 1561-1564.
2. N. Menyuk, K. Dwight, J. W. Pierce, *Appl. Phys. Lett.*, 1972, **21**, 159-161.
3. J. L. Sommerdijk, *Journal of Lumin.*, 1973, **6**, 61-67.
4. R. Kapoor, C. S. Friend, A. Biswas, P. N. Prasad, *Opt. Lett*. 2000, **25**, 338-340.
5. S. Heer, O. Lehmann, M. Haase, H. U. Gudel, *Angew. Chem. Int. Ed*., 2003, **42**, 3179-3182.
6. F. Auzel, *Chem. Rev.*, 2004, **104**, 139-173.
7. F. Vetrone, J. C. Boyer, J. A. Capobianco, *J. Appl. Phys.*, 2004, **96**, 661-667.
8. T. Hirai, T. Orikoshi, *J. Colloid Interf. Sci.,* 2004, **269**, 103-108.
9. F. Wang, X. G. Liu, *Chem. Soc. Rev.*, 2009**, 38**, 976-989.
10. N. Liu, W. P. Qin, G. S. Qin, T Jiang, D. Zhao, *Chem. Commun.*, 2011, **47**, 7671-7673.
11. Q. Liu, Y. Sun, T. S. Yang, W. Feng, C. G. Li, F. Y. Li, *J. Am. Chem. Soc*., 2011, **133**, 17122-17125.
12. Y. H. Wang, L. Bao, Z. H. Liu, D. W. Pang, *Anal. Chem*., 2011, **83**, 8130-8137.
13. C. Wang, L. Cheng, Z. Liu, *Biomaterials*, 2011, **32**, 1110-1120.
14. S. S. Cui, D.Y. Yin, Y. Q. Chen, Y. F. Di, H. Y. Chen, Y. X. Ma, S. Achilefu, Y. Q. Gu, *ACS Nano*., 2013, **7**, 676-688.
15. Y. S. Liu, D. T. Tu, H. M. Zhu, X.Y. Chen, *Chem. Soc. Rev.*, 2013, **42**, 6924-6958.

16. S. L. Gai, C. X. Li, P. P. Yang, J. Lin, *Chem. Rev*., 2014, **114**, 2343-2389.
17. J. B. Zhao, Z. D. Lu, Y. D. Yin, C. McRae, J. A. Piper, J. M. Dawes, D. Y. Jin, E. M. Goldys, *Nanoscale*, 2013, **5**, 944-952.
18. H. Na, K. Woo, K. Lim, H. S. Jang, *Nanoscale*, 2013, **5**, 4242-4251.
19. N. Niu, F. He, S. L. Gai, C. X. Li, X. Zhang, S. H. Huang, P. P. Yang, *J. Mater. Chem.*, 2012, **22**, 21613-21623.
20. Y. F. Wang, G. Y. Liu, L. D. Sun, J. W. Xiao, J. C. Zhou, C. H. Yan, *ACS Nano*., 2013, **7**, 7200-7206.
21. G. Y. Chen, T. Y. Ohulchanskyy, S. Liu, W. C. Law, F. Wu, M. T. Swihart, H. Agren, P. N. Prasad, *ACS Nano*., 2012, **6**, 2969-2977.
22. J. Shen, G. Y. Chen, A. M. Vu, W. Fan, O. S. Bilsel, C. C. Chang, G. Han, *Adv. Optical Mater*., 2013, **1**, 644-650.
23. X. J. Xie, N. Y. Gao, R. R. Deng, Q. Sun, Q. H. Xu, X. G. Liu, *J. Am. Chem. Soc*., 2013, **135**, 12608-12611.
24. H. L. Wen, H. Zhu, X. Chen, T. F. Hung, B. L. Wang, G. Y. Zhu, S. F. Yu, F. Wang, *Angew. Chem*. Int. Ed., 2013, **125**, 1-6.
25. X. M. Li, R. Wang, F. Zhang, L. Zhou, D. K. Shen, C. Yao, D. Y. Zhao, *Sci. Rep*., 2013, **3**, 3536.
26. M. K. G. Jayakumar, N. M. Idris, K. Huang, Y. Zhang, *Nanoscale*, 2014, **6**, 8441-8443.
27. Z. Q. Li, Y. Zhang, S. Jiang, *Adv. Mater*., 2008**, 20**, 4765-4769.
28. H. Guo, Z. Q. Li, H. S. Qian, Y. Hu, I. N. Muhammad, *Nanotechnology*, 2010, **21**, 125602.
29. H. S. Qian, Y. Zhang, *Langmuir*, 2008, **24**, 12123-12125.
30. H. Zhang, Y. J. Li, Y. C. Lin, Y. Huang, X. F. Duan, *Nanoscale*, 2011, **3**, 963-966.
31. C. Z. Zhao, X. G. Kong, X. M. Liu, L. P. Tu, F. Wu, Y. L. Zhang, K. Liu, Q. H. Zeng, H. Zhang, *Nanoscale*, 2013, **5**, 8084-8089.
32. A. X. Yin, Y. W. Zhang, L. D. Sun, C. H. Yan, *Nanoscale*, 2010, **2**, 953-959.
33. S. Heer, K. Kömpe, H. U. Güdel, M. Haase, *Adv. Mater*. 2004, **16**, 2102-2105.
34. J. H. Zeng, J. Su, Z. H. Li, R. X. Yan, Y. D. Li, *Adv. Mater.* 2005, **17**, 2119-2123.
35. F. Vetrone, R. Naccache, V. Mahalingam, C. G. Morgan, J. A. Capobianco, *Adv. Funct. Mater*. 2009, **19**, 2924-2929.
36. R. Naccache, F. Vetrone, V. Mahalingam, L. A. Cuccia, J. A. Capobianco, *Chem. Mater*. 2009, **21**, 717-723.
37. M. Haase, H. Schafer, *Angew. Chem. Int. Ed.,* 2011, **50**, 5808-5829.
38. A. Aebischer, M. Hostettler, J. Hauser, K. Kramer, T. Weber, H. U. Gudel, H. B. Burgi, *Angew. Chem. Int. Ed.,* 2006, **45**, 2802-2806.
39. F. Shi, J. S. Wang, D. S. Zhang, G. S. Qin, W. P. Qin, *J. Mater. Chem.*, 2011, **21**, 13413-13421.
40. B. Zhou, L. L. Tao, Y. H. Tsang, W. Jin, *J. Mater. Chem. C*, 2013, **1**, 4313-4318.